



STOCHASTIC MODEL OF NEAR-FAULT GROUND MOTION SIMULATION AND RELIABILITY ASSESSMENT OF STRUCTURES

Guohai Chen⁽¹⁾, Dixiong Yang⁽²⁾

⁽¹⁾ Postdoctoral fellow, School of Civil Engineering, Dalian University of Technology, Dalian, China, chengh_414@dlut.edu.cn

⁽²⁾ Professor, Department of Engineering Mechanics, Dalian University of Technology, Dalian, China, yangdx@dlut.edu.cn

Abstract

The forward directivity and fling-step effects of fault rupture generally result in the distinct long-period pulses in velocity time histories of near-fault ground motions. Such velocity pulses present large amplitude and long period, and easily result in the nonlinear seismic responses and damage to building structures. Besides, seismic ground motions also possess strong randomness and time-frequency nonstationary characteristic. Therefore, the stochastic model of near-fault ground motions and the reliability assessment of structures play crucial roles in performance-based earthquake engineering. This study focuses on the stochastic simulation of near-fault ground motions and the efficient method for assessing first passage dynamic reliability for structures. Firstly, the stochastic model of near-fault ground motion simulation is established. In the model, the velocity time history with strongest pulse is first generated based on the orthogonal horizontal components by using wavelet analysis. The velocity pulse is extracted from the time-history with the strongest pulse and fitted to the M-P pulse model in the sense of least square. The low-frequency acceleration time-history is achieved by taking derivation of the velocity pulse analytically. Secondly, the probability density integral equation (PDIE) controlling the propagation of randomness from stochastic ground motion to structural response is derived based on the principle of probability conservation. By using the techniques of partition of probability space and smoothing of Dirac delta function, the direct probability integral method (DPIM) is proposed to efficiently solve PDIE and obtain the probability density functions of stochastic responses of structures. Moreover, the DPIM is extended to assess the first passage dynamic reliability of building structures with nonlinear hysteretic behavior. Finally, numerical examples demonstrate the effectiveness of established stochastic model and efficiency of proposed method for seismic reliability assessment of hysteretic frame structure in near-fault area. The effect of velocity pulses on the failure probability of structures is also scrutinized.

Keywords: Near-fault ground motions; stochastic model; velocity pulse; direct probability integral method; dynamic reliability of structures



1. Introduction

Near-fault ground motions are closely related with the rupturing mechanism of the fault, and generally present the effects of forward directivity and fling-step. Both the effects may cause the distinct long-period pulse in velocity time histories [1]. Such velocity pulses possess larger amplitude and long duration and exhibit large uncertainty, which usually result in the nonlinear responses and damage for building structures. Therefore, the reliability assessment of building structures subject to near-fault ground motions is critical for seismic design of structures.

Many studies on the near-fault pulse model have been carried out. Commonly, a simple velocity waveform, such as the trigonometric functions [2] and wavelet function [3], is used to fit the long-period velocity pulse. Dickinson and Gavin [4] suggested a statistical analysis method for ground motion records under a seismic hazard level and a geographic region, and obtained the probability distribution of the parameters that describe the low- and high-frequency stochastic contents of ground motions. By taking the orientation of the strongest pulse into account, Yang and Zhou [5] proposed a stochastic synthesis model of near-fault pulse-like ground motion, in which the velocity pulse was described by single Gabor wavelet. Dabaghi and Der Kiureghian [4] suggested another model by combining M-P pulse model and filtered Gaussian random process, which can reflect the nonstationarity of ground motions. In above models, however, a lot of random variables are inevitably introduced to reproduce the near-fault impulsive ground motions. Such models have to make the Monte Carlo simulation (MCS) to assess the dynamic reliability of structures.

Recently, authors proposed an efficient method, namely direct probability integral method (DPIM) [7], for stochastic response analysis of structures. This method is based on the probability density integral equation governing the randomness propagation of structures. With this idea, the DPIM can be easily extended to reliability analysis, including static reliability and dynamic reliability. This study aims to evaluate the dynamic reliability of building structures under near-fault ground motions. For this purpose, firstly, this work establishes a stochastic model for near-fault impulsive ground motion, which represented the velocity pulse and time-frequency non-stationarity of near-fault ground motions. Then, the dynamic reliability of building is assessed by utilized the DPIM. Finally, the effects of velocity pulse parameters on dynamic reliability of structures are also scrutinized.

2. Stochastic model of near-fault ground motions

2.1 Long-period velocity pulse

In this paper, the long-period velocity pulse is expressed by the M-P pulse model proposed by Mavroeidis and Papageorgiou [2] that is

$$V_p(t; T_p, N_c, T_{pk}, \varphi) = \frac{PGV}{2} \left[1 + \cos\left(\frac{2\pi(t - T_{pk})}{T_p N_c}\right) \right] \cdot \cos\left(2\pi \frac{t - T_{pk}}{T_p} - \varphi\right), \quad T_{pk} - \frac{T_p N_c}{2} \leq t \leq T_{pk} + \frac{T_p N_c}{2} \quad (1)$$

in which T_p , N_c , T_{pk} and φ represent the pulse period, number of circles in the pulse, the time of peak value of the velocity pulse, respectively; the attenuation of PGV is fitted by using the regression formula presented by Bary and Rodriguez-Marekis [1]

$$\ln(PGV) = a + bM_w + c \ln(R_{rup}^2 + d^2) + \sigma_{\ln PGV} \quad (2)$$

where M_w is the moment magnitude; R_{rup} denotes the closest distance from the recording site to the ruptured area, which is considered as the fault distance in this study; and c_1 , c_2 , c_3 and c_4 are the regression parameters; σ represents the regression residual, respectively.



2.2 High-frequency components

The residual acceleration time series can be generated by extracting the domain pulse and differentiating the residual velocity history. In this study, a random variable based spectral representation method [8] is employed to simulate the residual stochastic nonstationary high-frequency components of near-fault ground motion, which is written as

$$a_{\text{res}}(t) = \sum_{k=0}^N \sqrt{S(t, \omega_k) \Delta \omega} \cdot [\cos(\omega_k t) X_k + \sin(\omega_k t) Y_k] \quad (3)$$

where $S(t, \omega_k)$ is the nonstationary power spectral density function of residual acceleration time history; $\Delta \omega = (\omega_u - \omega_l) / N$ denotes the frequency step size; $\omega_k = \omega_l + k(\omega_u - \omega_l) / N$ means the discrete frequency; X_k and Y_k are the orthogonal random variables, which can be defined as a random function with one elementary random variable γ as follows

$$X_k = \sqrt{2} \cos(k\gamma + \frac{\pi}{4}), \quad Y_k = \sqrt{2} \sin(k\gamma + \frac{\pi}{4}) \quad (4)$$

in which the elementary random variable γ is uniformly distributed within $[-\pi, \pi]$.

In Eq. (3), a modified K-T (Kanai-Tajimi) spectrum with high-pass filter modulated by a random variable based envelope function in Yang and Zhou (2015) is used to express the nonstationary spectral function, namely

$$S(t, \omega) = |e(t)|^2 G(\omega) S_{\text{K-T}}(\omega) \quad (5)$$

where $e(t)$, $G(\omega)$ and $S_{\text{K-T}}(\omega)$ indicate the envelope function, Butterworth filter, K-T spectrum, respectively. To present the variability of envelope function, the following stochastic envelope function with three random parameters [5] is also adopted

$$S_{\text{K-T}}(\omega) = \frac{1 + 4\xi_g^2 \omega^2 / \omega_g^2}{(1 - \omega^2 / \omega_g^2)^2 + 4\xi_g^2 \omega^2 / \omega_g^2} S_0, \quad G(\omega) = \frac{\omega^{2N}}{\omega^{2N} + \omega_h^{2N}} \quad (6)$$

$$e(\alpha, \beta, t_{pk}; t) = \begin{cases} 0 & t \leq t_0 \\ \left(\frac{t - t_0}{t_{pk}} \right)^\alpha & t_0 \leq t \leq t_0 + t_{pk} \\ e^{-\beta(t - t_0 - t_{pk})} & t \geq t_0 + t_{pk} \end{cases} \quad (7)$$

In Eq. (7) the parameter t_0 describes the initial instant of non-zero ground motion; t_{pk} denotes the time of peak value of residual acceleration; α and β are the power exponents corresponding to the ascending and descending segments. In this model, the envelope parameters t_{pk} , α and β are considered as random variables.

Consequently, the stochastic velocity time history $V_s(t)$ of ground motion scaled by the peak of residual velocity history V_{res} , and the high-frequency acceleration $a_s(t)$ of the near-fault ground motion can then be obtained by differentiating the scaled velocity time series. Finally, the acceleration time series with the strongest pulse can be generated by the superposition of the high-frequency acceleration and the low-frequency counterpart $a_p(t)$ achieved from the velocity pulse function shown in Eq. (1).

3 Parameters estimation and synthesis of ground motions

3.1 Model parameters identification



As stated in Section 2.1, the velocity time history with strongest velocity pulse is first generated based on the two orthogonal components of fault-normal and fault-parallel directions by means of wavelet transformation. Then, the long-period velocity pulse time history can be extracted from the generated velocity time history with strongest pulse by utilizing a low pass filter. Finally, the pulse parameters in Eq. (1) can be identified by the nonlinear least square method:

$$(\hat{T}_p, \hat{N}_c, \hat{T}_{pk}, \hat{\phi}, \hat{\sigma}_{\ln PGV}) = \arg \min \sum_{i=1}^{N_t} [v(t_i) - v_p(t_i; T_p, N_c, T_{pk}, \phi, \sigma_{\ln PGV})]^2 \quad (8)$$

To identify the parameters of envelop function, the instantaneous amplitude $\tilde{a}(t)$ of residual acceleration time histories $\ddot{x}(t)$ are first solved by combining with its Hilbert transformation $\ddot{x}_H(t)$, that is

$$\tilde{a}(t) = \sqrt{\ddot{x}(t)^2 + \ddot{x}_H(t)^2} \quad (9)$$

Then, the multimodal point method [5] is adopted to find the local maximal value of instantaneous amplitude in Eq. (9) so as to form the p th level envelope $\hat{a}^{(p)}(t)$. Furthermore, the obtained envelope $\hat{a}^{(p)}(t)$ is fitted with envelope function $e(t)$ in Eq. (7) to identify the envelope parameters in a least square sense:

$$(\hat{t}_{pk}, \hat{\alpha}, \hat{\beta}) = \arg \min \sum_{i=1}^{N_t} [\hat{a}^{(p)}(t_i) - e(t_i; t_{pk}, \alpha, \beta)]^2 \quad (10)$$

Figure 1 shows the 2–5th envelope lines of residual acceleration time history recorded at station TCU031. It is seen that third ($p=3$) and fourth ($p=4$) level envelope present the change of instantaneous amplitude of residual acceleration. Therefore, the third ($p=3$) level envelope is adopted for all of records selected in this paper.

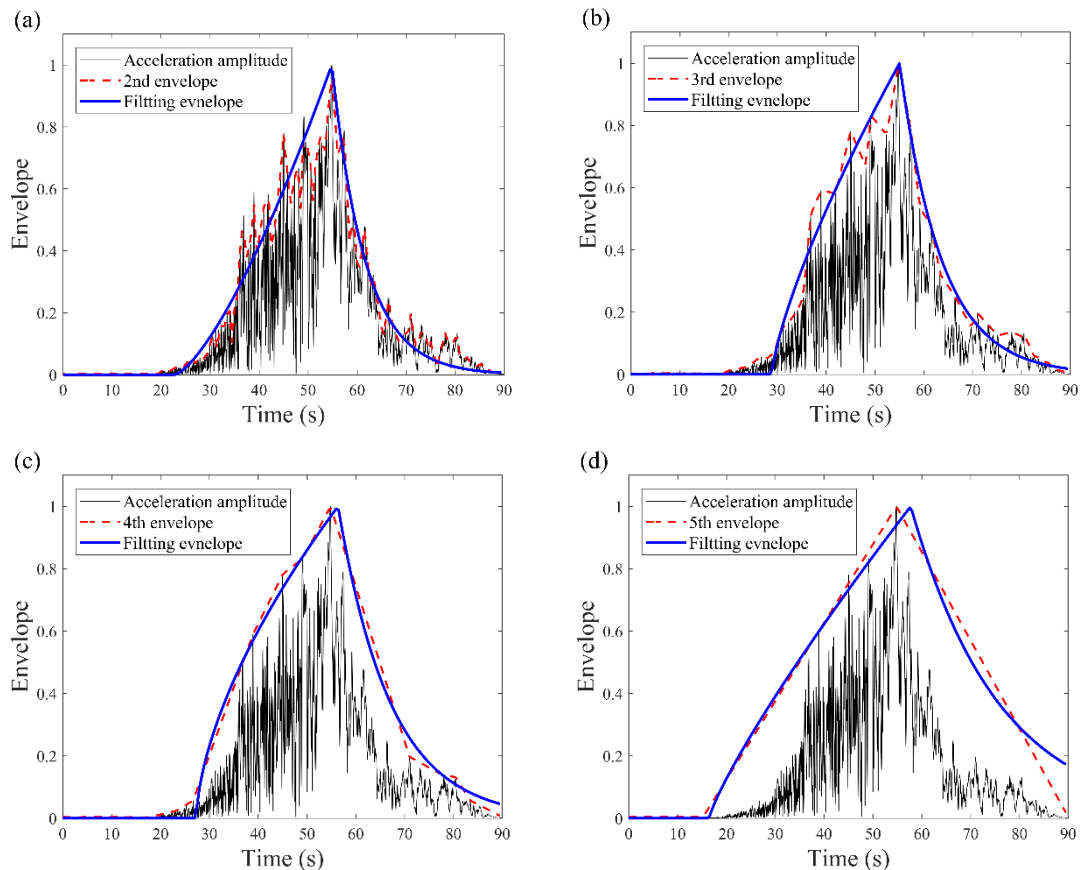


Fig.1 Envelope of the acceleration time history with strongest pulse at TCU031 station



In this study, the model parameters are identified by 34 near-fault pulse-like records with the rupture forward directivity effect in the range of fault distance $R_{rup} \leq 30$ km in Chichi earthquake event ($M_w=7.6$). Table 1 shows the probability distribution of model parameters and its mean value and standard deviation, in which model parameter for high frequency γ is uniformly distributed within $[-\pi, \pi]$ to represent the residual high-frequency stochastic process, as shown in Eq. (3).

Table 1 Probability distribution of parameters of stochastic ground motion model

Parameter type	Parameters	Distribution	Bounds	Mean	Std. D
Pulse parameters	T_p	Normal	[2.39, 10.84]	6.72	1.89
	N_c	Lognormal	[1.10, 4.23]	2.35	0.74
	T_{pk}	Normal	[7.04, 51.60]	25.69	10.05
	φ	Uniform	[0, 2π]	2.32	1.95
	$\sigma_{\ln PGV}$	Normal	[-0.6, 0.6]	0.00	0.25
Envelope parameters	t_{pk}	Normal	[10.43, 47.58]	25.63	9.18
	α	Lognormal	[0.22, 14.14]	2.59	3.34
	β	Lognormal	[0.03, 0.41]	0.09	0.07
High-frequency parameter	γ	Uniform	$[-\pi, \pi]$	0.00	$\pi^2/3$

3.1 Synthesis of near-fault pulse-like ground motions

After obtaining the probability distribution of model parameters, the representative ground motions can be generated by means of the point selection technology [8, 10]. In this work, a new point selection technique based on the generalized F-discrepancy (GF-discrepancy) [10] is adopted, which is suitable for the cases of non-normal distributed parameters.

Accordingly, the GF-discrepancy is defined as [10]

$$D_{GF} = \max_{1 \leq i \leq s} \left\{ \sup |F_{N,i}(\theta) - F_i(\theta)| \right\} \quad (11)$$

where $F_i(\theta)$ is the marginal CDF of the i th random variable; $F_{N,i}(\theta)$ is the empirical CDF considering the effects of assigned probability

$$F_{n,i}(\theta) = \sum_{q=1}^N P_q \cdot I\{\theta_{q,i} < \theta\} \quad (12)$$

The first step is to generate the N initial point set $\theta_q = (\theta_{q,1}, \theta_{q,2}, \dots, \theta_{q,s})$, $q=1, 2, \dots, N$ from a Sobol set $I_n = \{(u_{q,1}, u_{q,2}, \dots, u_{q,s}), q=1, 2, \dots, N\}$ over a unit hypercube by

$$\theta_{m,i} = F_i^{-1}(u_{m,i}) \quad (13)$$

where $F_i^{-1}(\bullet)$ denotes the inverse CDF of the i th random variable. To ensure that the weights of numerical integration, that is, assigned probability are close to each other, then the following transformation is performed in each dimension [10]



$$\theta'_{m,i} = F_i^{-1} \left(\sum_{q=1}^N \frac{1}{N} \cdot I\{\theta_{q,i} < \theta'_{m,i}\} + \frac{1}{2} \cdot \frac{1}{N} \right) \quad (14)$$

The second step is to calculate the assigned probability and transform point set so as to minimize the assigned probability of point set. Hence, the point set $\theta'_q = (\theta'_{q,1}, \theta'_{q,2}, \dots, \theta'_{q,s})$, $q = 1, 2, \dots, N$ are further transformed as [10]

$$\theta''_{m,i} = F_i^{-1} \left(\sum_{q=1}^N P_q \cdot I\{\theta'_{q,i} < \theta''_{m,i}\} + \frac{1}{2} \cdot P_m \right) \quad (15)$$

By using the new points selection technique, the final representation points with smaller GF-discrepancy can be determined as $\theta''_q = (\theta''_{q,1}, \theta''_{q,2}, \dots, \theta''_{q,s})$.

Figure 2 illustrates the velocity and acceleration time histories at stations of TCU031 and TCU051. From these figures, one can observe that the velocity pulses can be effectively extracted from the velocity time histories of actual records, and the synthetic acceleration time histories are matched with the original records.

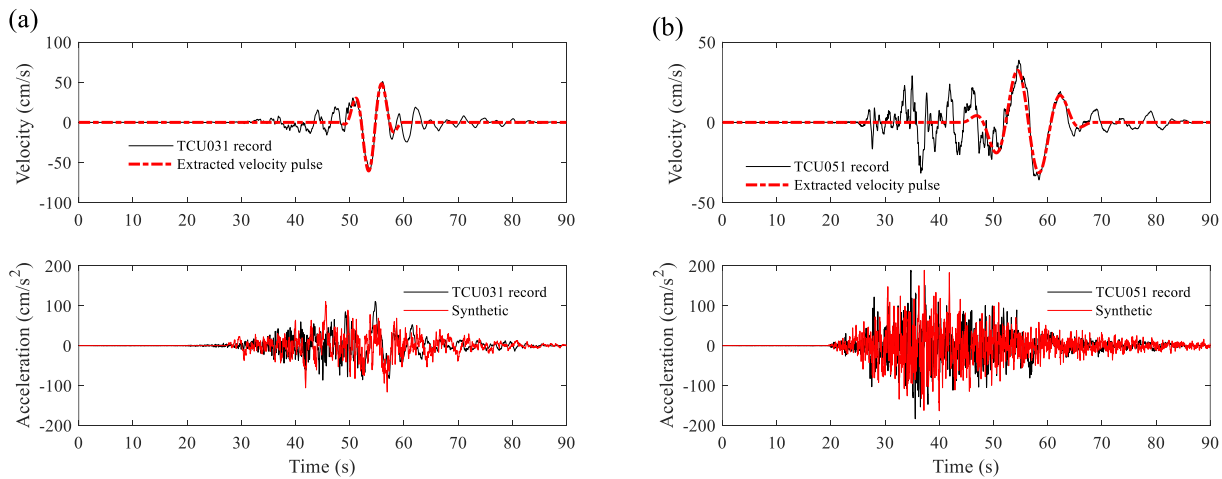


Fig. 2 Velocity and acceleration time histories at the station of (a) TCU031; (b) TCU051

4 Dynamic reliability assessment via direct probability integral method

3.1 Probability density integral equation

A nonlinear MDOF system subjected to the ground motion acceleration can be described by the following differential motion equation (physical mapping)

$$\mathbf{M}\ddot{\mathbf{X}} + \mathbf{C}\dot{\mathbf{X}} + \mathbf{f}(\mathbf{X}) = -\mathbf{M}\mathbf{I}\ddot{u}_g(\Theta, t) \quad (16)$$

with the deterministic initial condition

$$\mathbf{X}(t)|_{t=0} = \mathbf{X}_0, \quad \dot{\mathbf{X}}(t)|_{t=0} = \dot{\mathbf{X}}_0 \quad (17)$$

where \mathbf{X} represents the relative displacement vector; \mathbf{M} and \mathbf{C} are mass and damping matrix, respectively; \mathbf{f} indicates the restoring force vector; \mathbf{I} is the $n \times 1$ unit column vector; $\ddot{u}_g(\Theta, t)$ is the acceleration history of near-fault impulsive ground motion described in Section 3; $\Theta = (T_p, N_c, T_{pk}, \varphi, \sigma_{lnPGV}, \alpha, \beta, t_{pk}, \gamma)$ denotes the



random parameters vector of near-fault ground motion; the deterministic initial condition \mathbf{X}_0 and $\dot{\mathbf{X}}_0$ are considered in this study.

Based on the principle of probability conservation of random event description, Chen and Yang [7] derived uniformly the probability density integral equations (PDIEs) for static and dynamic structural systems, respectively. In this study, the structure is subjected to the seismic ground motions. The PDIE of dynamic version, therefore, is expressed as follows

$$p_{\mathbf{x}}(\mathbf{x}, t) = \int_{\Omega_{\theta}} p_{\theta}(\theta) \delta[\mathbf{x} - \mathbf{g}(\theta, t)] d\theta \quad (18)$$

where $\delta(\cdot)$ is the Dirac delta function; $\mathbf{g}(\theta, t)$ denotes the solution of physical equation in Eq. (17); $p_{\theta}(\theta)$ is the joint probability density function of random parameters θ ; Ω_{θ} is the distribution domain of θ .

If the certain component of responses $X(t)$ is concerned, the PDIE in Eq. (18) can be reduced according to the property of Dirac delta function, that is

$$p_X(x, t) = \int_{\Omega_{\theta}} p_{\theta}(\theta) \delta[x - g(\theta, t)] d\theta \quad (19)$$

3.2 Direct probability integral method

To solve the PDIE in Eq. (19), the direct probability integral method (DPIM) was proposed by means of the partition of probability space and smoothing of Dirac delta function in previous work [7].

By using the partition of probability space, the representative point set can be generated according GF-discrepancy based point selection method, then the representative ground motions can be synthesized. The PDIE in Eq. (19), therefore, can be written as [7]

$$p_X(x, t) \approx \sum_{q=1}^N \left\{ \delta[x - g(\theta_q, t)] P_q \right\} \quad (20)$$

where the assigned probability of a representative point θ_q is obtained by numerically solving the following integration

$$P_q = \int_{\Omega_{\theta, q}} p_{\theta}(\theta) d\theta \quad (21)$$

In numerical integration, the non-smooth Dirac delta function involved in Eq. (19) needs to be approximated by using smooth function. The previous work showed that the Gaussian function is an appropriate to treat this problem. Consequently, Eq. (20) can be further expressed as follows [7]

$$p_X(x, t) \approx \sum_{q=1}^N \left\{ \frac{1}{\sqrt{2\pi}\sigma} e^{-[x - g(\theta_q, t)]^2 / 2\sigma^2} P_q \right\} \quad (22)$$

in which σ is the smoothing parameters. When $\sigma \rightarrow 0$, the smooth function $\hat{\delta}(y; \sigma)$ tends to Dirac delta function, i.e., $\delta(y) = \lim_{\sigma \rightarrow 0} \hat{\delta}(y; \sigma)$.

3.2 First-passage dynamic reliability analysis based on DPIM

Based on the first passage failure criterion, the dynamic reliability of structures is defined as [9, 11]

$$P_r(t) = \Pr \{ X(\tau) \in \Omega_s, 0 < \tau \leq t \} \quad (23)$$

where Ω_s denotes the safety domain.

According to the definition in Eq. (23), once the response crosses the safety boundary in certain moment, the system would be failure. Therefore, a random process can be viewed a serial system over the time domain, that is, the structure fails when the maximum of response in time interval $(0, t]$ exceeds the threshold. Then, the reliability of structure at instant t can be expressed as [9]



$$P_r(t) = \Pr \left\{ \bigcap_{0 < \tau \leq t} X(\Theta, \tau) \in \Omega_s \right\} = \Pr \{ X_{\max} < b \} \quad (24)$$

where b is the given threshold; $X_{\max} = h(\Theta) = \max_{0 < \tau \leq t} \{X(\Theta, \tau)\}$, which is a mapping $\mathcal{H}: \Theta \rightarrow X_{\max}$. The stochastic response $Y(t)$ is transformed into the random variable X_{\max} , then the performance can be rewritten as follows

$$Z = g(\Theta) = b - h(\Theta) \quad (25)$$

In the context of the DPIM, the PDF of performance in Eq. (25) can be attained by

$$p_Z(z) \approx \sum_{q=1}^N \left\{ \frac{1}{\sqrt{2\pi}\sigma} e^{-[z-g(\Theta)]^2/2\sigma^2} P_q \right\} \quad (26)$$

Thus, the dynamic reliability at instant t can also be calculated by

$$P_r(t) = \Pr[Z > 0] = \int_0^{\infty} p_Z(z) dz \quad (27)$$

This approach transforms the stochastic process into a random variable to obtain the dynamic reliability of structures.

5 Numerical example of dynamic reliability analysis for hysteretic frame structure

In this section, a two-span 20-story shear frame subjected to stochastic ground motion, as illustrated in Fig. 3, is considered. The floor lumped masses of the frame are from the bottom to top floor are taken as: $m_1 = m_2 = 4.5$, $m_3 = \dots = m_{12} = 4.3$, $m_{13} = \dots = m_{17} = 4.1$, $m_{18} = m_{20} = 3.9$ (10^5 kg); and the initial lateral inter-story stiffnesses: $k_1 = k_2 = 3.5$, $k_3 = \dots = k_{12} = 3.2$, $k_{13} = \dots = k_{17} = 3.0$, $k_{18} = k_{20} = 2.8$ (10^8 N/m).

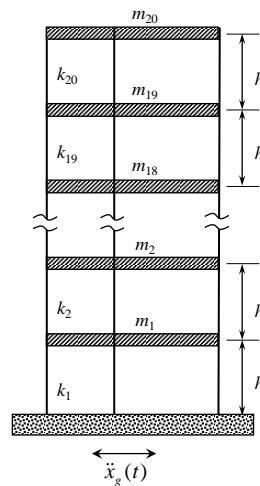


Fig. 3 Two-span 20-story shear frame subjected to earthquake ground motion

Assume that the failure occurs once the inter-story drift exceeds prescribed threshold, i.e., $b = 0.06$ m. The stochastic inter-story drift is denoted as $\mathbf{Y}(\Theta, t) = [Y_1(\Theta, t), Y_2(\Theta, t), \dots, Y_{20}(\Theta, t)]$, in which $Y_1(\Theta, t) = X_1(\Theta, t)$; $Y_i(\Theta, t) = X_i(\Theta, t) - X_{i-1}(\Theta, t)$, $i = 2, \dots, 20$. Therefore, the performance function can also be given by the mapping

$$Z = g(\Theta, t) = b - \max_{1 \leq i \leq 20} \{Y_i(\Theta, t)\} \quad (28)$$

where the $X_i(\Theta, t)$ indicate the i th floor displacement of the frame, which can be calculated by the physical mapping:



$$\mathbf{M}\ddot{\mathbf{X}} + \mathbf{C}\dot{\mathbf{X}} + \alpha\mathbf{K}\mathbf{X} + (1-\alpha)\mathbf{K}\mathbf{Z}_h = -\mathbf{M}\ddot{\mathbf{x}}(\mathbf{\Theta}, t) \quad (29)$$

in which $\mathbf{M}=\text{diag}(m_1, m_2, \dots, m_{20})$ denotes the mass matrix; \mathbf{K} is the initial stiffness matrix; $\mathbf{C}=\alpha_1\mathbf{M}+ \alpha_2\mathbf{K}$ ($\alpha_1=0.4602 \text{ s}^{-1}$, $\alpha_2=0.0041 \text{ s}$) is adopted; $\mathbf{Z}_h=(Z_{h,1}, Z_{h,2}, \dots, Z_{h,20})^T$ denotes the hysteretic displacement, which is described by Bouc-Wen model; α is the ratio of the final tangent stiffness to initial stiffness in this model, and the other parameters are be found in Ref. [7]

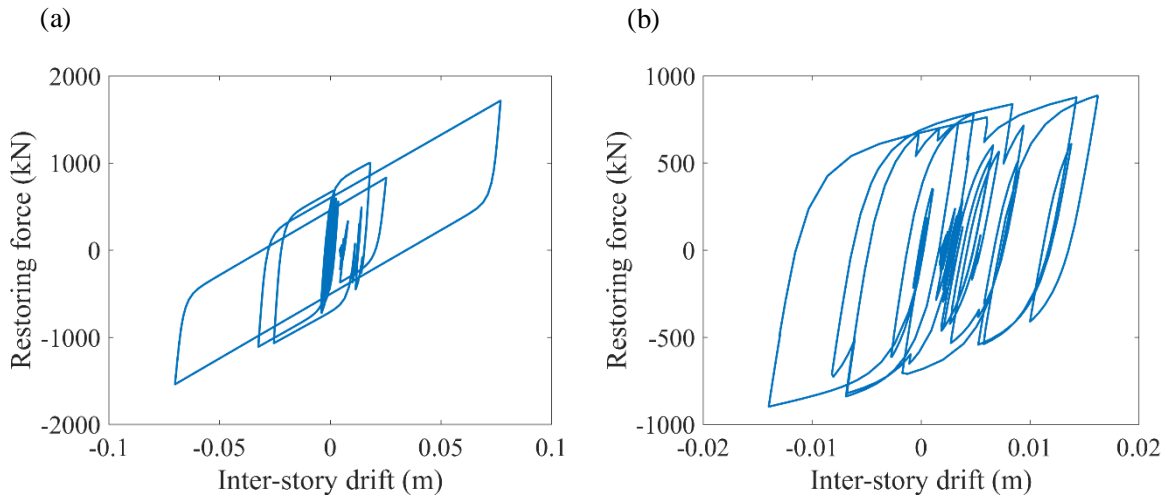


Fig. 4 Restoring curves of structure under (a) pulse-like ground motion; (b) non-pulse ground motion

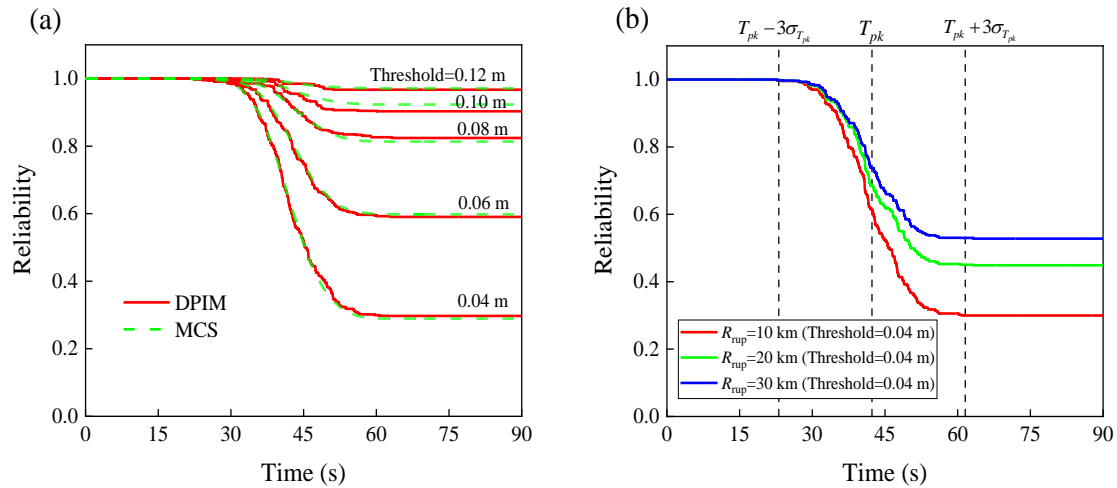


Fig. 5. Dynamic reliability under different (a) thresholds and (b) fault distances R_{rup}

Figure 4 (a) and (b) illustrate the curves of restoring force versus inter-story drift of the structure subjected to near-fault pulse-like and non-pulse-like ground motion, respectively. It is seen that the velocity pulse can result in larger inter-story drift than the non-pulse like ground motion. It presents the importance of the study on reliability of structures under near-fault pulse-like ground motions.

The dynamic reliability of tall building under different threshold values (0.04, 0.06, 0.08, 0.10, 0.12 m) are depicted in Fig. 5(a). From this figure, it shows that the DPIM obtains agree results with those by MCS, and demonstrates the good accuracy of proposed method. Fig. 5(b) examines the effect of occurrence instant T_{pk} of velocity pulse for near-fault ground motion with different fault distances on dynamic reliability of the structure. It is observed that the reliability decreases remarkably from 1 to the minimum value in the time



interval $[T_{pk} - 3\sigma_{T_{pk}}, T_{pk} + 3\sigma_{T_{pk}}]$, and the velocity pulse of near-fault ground motion affects significantly the dynamic reliability of structures, especially for the structures located in the area closer to the fault.

6 Conclusions

In this work, an efficient framework is proposed to assess the dynamic reliability of structures subjected to near-fault pulse-like ground motions. Firstly, a stochastic synthesis model is established on the basis of near-fault ground motion records. Then, the direct probability integral method is employed to perform dynamic reliability analysis for nonlinear structures. As a numerical example, the dynamic reliability of the 20-story shear frame building is achieved. Several main conclusions are drawn as follows:

- (1) The velocity pulse has a critical effect on failure of structures in the area closer to the rupturing fault.
- (2) The variability of velocity pulse parameters plays an important role and cannot be neglected in structural dynamic reliability analysis.
- (3) The proposed DPIM is an efficient and accurate method for dynamic reliability assessment of nonlinear structure subjected to near-fault pulse-like ground motions.

Acknowledgments

The supports of the National Natural Science Foundation of China (Grant No. 11772079), the National Key R&D Program of China (Grant No. 2016YFB0201600) and the China Postdoctoral Science Foundation (Grant No. 2019M661088) are much appreciated.

References

- [1] Bray JD, Rodriguez-Marek A (2004): Characterization of Forward-directivity Ground Motions in the Near-fault Region, *Soil Dynamics and Earthquake Engineering*, **24**(11), 815–828.
- [2] Mavroeidis GP, Papageorgiou AS (2003): A Mathematical Representation of Near-fault Ground Motions, *Bulletin of the Seismological Society of America*, **93**(3), 1099–1131.
- [3] Baker JW (2007): Quantitative Classification of Near-fault Ground Motions Using Wavelet Analysis, *Bulletin of the Seismological Society of America*, **97**(5), 1486–1501.
- [4] Dickinson BW, Gavin HP (2011): Parametric Statistical Generalization of Uniform-hazard Earthquake Ground Motions, *Journal of Structural Engineering*, **137**(3), 410–422.
- [5] Yang DX, Zhou JL (2015): A Stochastic Model and Synthesis for Near-fault Impulsive Ground Motions, *Earthquake Engineering & Structural Dynamics*, **44**(2), 243–264.
- [6] Dabaghi M, Der Kiureghian A (2017): Stochastic Model for Simulation of Near-fault Ground Motions, *Earthquake Engineering & Structural Dynamics*, **46**(6), 963–984.
- [7] Chen GH, Yang DX (2019): Direct probability integral method for stochastic response analysis of static and dynamic structural systems, *Computer Methods in Applied Mechanics and Engineering*, **357**:112612.
- [8] Liu ZJ, Liu W, Peng YB (2016): Random Function based Spectral Representation of Stationary and Non-stationary Stochastic Processes, *Probabilistic Engineering Mechanics*, **45**, 115–126.
- [9] Li J, Chen JB (2009): *Stochastic Dynamics of Structures*, John Wiley & Sons, Singapore.
- [10] Chen JB, Yang JY, Li J (2016): A GF-discrepancy for point selection in stochastic seismic response analysis of structures with uncertain parameters, *Structural Safety*, **59**, 20–31.
- [11] Melchers RE, Beck AT (2018): *Structural Reliability Analysis and Prediction*, John Wiley & Sons.